RSC Advances

COMMUNICATION

Effect of surface properties in protein corona development on mesoporous silica nanoparticles†

Cite this: *RSC Adv.*, 2014, **4**, 29134

Alden M. Clemments,[a] Carlos Muniesa,[b] Christopher C. Landry*[a] and Pablo Botella*[b]

Received 11th April 2014
Accepted 18th June 2014

DOI: 10.1039/c4ra03277b

www.rsc.org/advances

The composition of the protein corona formed on mesoporous silica nanoparticles with several surface modifications was characterized. Low MW serum proteins were preferentially adsorbed, and PEGylated nanoparticles did not adsorb protein regardless of PEG chain length.

Nanomedicine is continuously providing new single and multifunctional alternatives to traditional pharmaceutical delivery and treatment, enhancing both therapeutic activity and selectivity to pathological tissues, as well as providing molecular recognition and biosensing features.[1,2] Unfortunately, the stability of most nanomaterials in biological fluids is still a challenge to be solved, and the incorporation of stable nanoparticles into the bloodstream provokes a strong reaction with serum proteins, lipids, and small molecules, forming a shell of aggregated compounds known as the protein corona.[3] The very high surface to volume ratio of nanomaterials dramatically boosts the adsorption process, changing their surface properties. This corona defines the biological identity of the nanomaterials and determines their final physiological fate. In the case of intravenous (iv) injection, protein adsorption drives nanoparticle uptake by monocytes and macrophages, leading to their distribution to the reticuloendothelial system (RES) and compromising their therapeutic efficacy.[4–7]

Independent of the nature of the nanomaterial, the protein corona grows in a few minutes over the particles and may evolve for several days.[8–10] It has a complex composition, often consisting of several dozens of proteins. Some of these proteins are loosely bound to particle surface (the "soft corona"), but, so far, most of the studies of this coating have been carried out over a short list of proteins firmly attached to particles forming the "hard corona", as this represents the protein signature of the nanomaterial in a given environment.[11–15] These studies have shown that the total protein concentration in biological fluids may change the composition of the corona, although, surprisingly, the concentration of a specific protein does not determine its presence in the biological layer (*e.g.*, human serum albumin is the most abundant protein in serum but is actually in minority around nanoparticles).[16,17] Moreover, the role of targeting molecules decorating the nanoparticle surface depends on this protein covering, as the interaction with specific receptors may be seriously hindered.[18]

Changing nanoparticle properties, such as material,[16] size,[12,19–21] and surface chemistry,[12,21,22] may alter the corona composition. Interestingly, the most widely applied strategy to block nonspecific protein adsorption on nanoparticles is to modify the surface by grafting linear chains of poly(ethylene glycol) (PEG).[21,23] In fact, different studies support that PEGylation of nanomaterials diminishes interaction with serum proteins, decreasing the rate of phagocytic uptake and increasing blood residence time.[24,25] Additionally, proteomics analysis has been performed on a wide range of organic and inorganic nanomaterials, such as polystyrene,[11,15,16] hydrogels,[22] carbon nanotubes,[26] gold,[9,21] SPIONs,[27] quantum dots,[28,29] and amorphous silica nanoparticles.[16,17,19,20,22] However, so far, no investigation has been reported on the protein corona on mesoporous silica nanoparticles (MSNs). In recent years, mesoporous silica materials have been considered to be excellent platforms for drug delivery systems.[30–33] The large internal porosity of MSNs favors the loading of significant quantities of therapeutic molecules within the pore channels. Furthermore, nanoparticle shape and size, as well as pore structure, can be easily tuned through various synthetic strategies.[34,35] Finally, the silanol-containing surface can be easily functionalized, introducing additional features that allow for stimuli-responsive controlled drug release.[36] Shi *et al.*[37] highlighted the effect of PEGylation of MSNs on human serum albumin binding and cellular responses, concluding that PEG grafting greatly decreased protein binding to MSNs as well as macrophage uptake. Nevertheless, additional work is needed to completely characterize the protein corona on MSNs, and how it evolves as a function of nanoparticle modification.

[a]*Department of Chemistry, University of Vermont, Burlington, VT 05405, USA. E-mail: christopher.landry@uvm.edu*

[b]*Instituto de Tecnología Química (UPV-CSIC), Av. Los Naranjos s/n, 46022 Valencia, Spain. E-mail: pbotella@itq.upv.es*

† Electronic supplementary information (ESI) available: Experimental details, the complete set of LC-MS data, and TEM images. See DOI: 10.1039/c4ra03277b

In the present work, we have carried out a complete compositional study of the protein corona adsorbed onto 50 nm MSNs after incubation (1 h) in Dulbecco's Modified Eagle's Medium containing 10% fetal bovine serum (FBS). A proteomic analysis using one-dimensional sodium dodecyl sulfate–polyacrylamide gel electrophoresis (SDS–PAGE) and electrospray liquid chromatography mass spectrometry (LC-MS) has been performed on the protein extract isolated from reacted nanoparticles. Quantitative results for most abundant proteins have been obtained by comparing proteomic distribution with thermogravimetric analysis (TGA) data. Furthermore, we have also investigated the influence of particle surface modification on the protein adsorption process by studying amine and carboxylate-modified MSNs, and we have used different chain length PEG molecules in order to evaluate the effect of PEGylation on particle reactivity.

Highly ordered mesoporous silica nanoparticles (MSNs) were synthesized, with BET surface area about 700–900 $m^2\ g^{-1}$. These MSNs were then used as the base material for further modifications (Fig. 1). The surface areas decreased slightly upon modification with amino- and carboxylate-silanes; however, the modification of the MSNs with PEG chains severely reduced the surface area. This is most likely due to surface shielding and pore blocking effects, consistent with the fact that the surface area for the material modified with a short PEG chain (241 $m^2\ g^{-1}$) was higher than for the long PEG chain (55 $m^2\ g^{-1}$). MSNs with average diameters of 50–55 nm (Table 1 and Fig. S1 and S2†) were obtained with low polydispersion, as characterized by transmission electron microscopy (TEM) and dynamic light scattering (DLS) techniques. Interestingly, the MSNs did not show significant changes in diameter as measured by DLS after exposure to 10% FBS solution, in contrast with the results of Monopoli *et al.* who described a 8–12% increase in the hydrodynamic diameter of amorphous silica nanoparticles after protein adsorption.[16] However, the latter study used much larger particles (~200 nm), which likely led to different amounts of protein being adsorbed.[20]

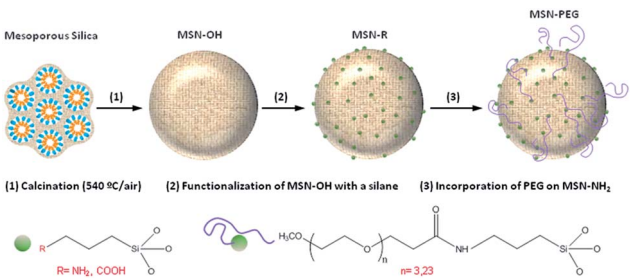

Fig. 1 Synthesis scheme for the materials used in these experiments.

Analysis using TGA, confirmed with elemental analysis, showed that the as-made materials (surface-modified but not yet exposed to protein) contained varying weight percentages of organic material. The total organic content of the amine- and carboxylate-modified MSNs was lower than that of the PEGylated MSNs, but this was primarily due to the increased mass of the PEG silanes. When calculated as mmol silane per g MSN, the trend is reversed, with more of the smaller silanes than the PEGs, which is consistent with the fact that the smaller silanes are able to access and modify the internal pore surfaces, while the larger PEG silanes primarily modify the external surface and the mouths of the pores, as described above. Finally, when the moles of each silane are scaled according to the available surface area (S_{BET}), which is more consistent with the portion of the MSN that interacts with the protein solution, the values of μmol m^{-2} are nearly the same, indicating that the surface coverages are similar regardless of the type of modification.

The base material had a zeta potential of −12.4 mV, which is consistent with a bare silica surface in solution. Modification with amine groups led to a less negative zeta potential (−7.9 mV) due to the protonation of amines in the neutral solution used for measurement; the fact that the value is not positive indicates that the surface has not been completely modified. Similarly, MSNs modified with PEG chains showed less negative zeta potentials due to the two-step process used to attach the PEG chains, which involved first modifying the surface with amines followed by reaction with *N*-hydroxysuccinimide (NHS)-modified PEG_3 or PEG_{24}. Thus the zeta potentials of the PEG-modified MSNs reflect the fact that both silanol and amine groups remain on the surface in addition to PEG. As expected, modification with carboxylate groups led to a more negative zeta potential (−15.4 mV).

Upon exposure to 10% FBS solution, the zeta potentials of the unmodified, $-NH_2$ modified, and –COOH modified MSNs became substantially less negative, consistent with the

Table 1 Characterization of as-prepared and FBS-exposed MSN samples

Sample	N_2 physisorption		Coverage		TGA (wt% organic)			Diameter[c] (nm)		ζ-potential (mV)		
MSN–X	S_{BET} ($m^2\ g^{-1}$)	d_{pore} (nm)	(mmol g^{-1})	(μmol m^{-2})[a]	As made	FBS-exposed[b]	Protein adsorbed	As made	FBS-exposed[b]	As made	FBS-exposed[b]	Δ
–OH	885	3.9	—	—	8.0	18.1	10.1	53.1 ± 27.0	50.6 ± 26.0	−12.4	−4.8	+7.6
$-NH_2$	734	3.1	2.43	3.31	8.4	22.8	14.4	51.6 ± 23.3	54.0 ± 27.3	−7.9	−4.0	+3.9
–COOH	813	3.4	2.10	2.58	14.4	16.7	2.3	50.5 ± 22.9	51.4 ± 23.0	−15.4	−10.2	+5.2
$-PEG_3-OCH_3$	241	2.7	0.87	3.61	23.5	23.3	—	49.9 ± 23.9	55.6 ± 27.0	−9.4	−8.7	+0.7
$-PEG_{24}-OCH_3$	55	1.9	0.24	4.36	31.1	28.9	—	51.4 ± 26.8	54.4 ± 27.0	−5.2	−5.9	−0.7

[a] Moles of organic group (μmol g^{-1}) divided by S_{BET} ($m^2\ g^{-1}$). [b] Particles placed in solutions containing 10% fetal bovine serum in phosphate-buffered saline. [c] Hydrodynamic diameter determined by dynamic light scattering.

formation of a protein corona. The corona led to a shielding effect that altered the surface charge of the particles, which has been reported by other authors using different materials.[9,22] In the case of the PEGylated MSNs, there was no significant change in zeta potential and therefore surface charge, leading to the conclusion that no significant protein corona had been formed. This was confirmed using thermogravimetric analysis (TGA) on MSNs before and after exposure to 10% FBS. Unmodified and $-NH_2$ modified MSNs showed significant amounts of adsorbed protein (10.1 and 14.4 wt%), with a lesser amount of protein adsorbed by the –COOH modified MSNs (2.3 wt%). In contrast, PEGylated MSNs showed no significant protein adsorption. Previous studies used long PEG chains,[23,26,37] but we show here that even a PEG trimer was sufficient to prevent the formation of a protein corona. This is relevant to the use of porous nanoparticles, because the decrease in surface area and therefore the extent of pore blockage was much smaller for $-PEG_3$ than for $-PEG_{24}$ modified MSNs.

The protein corona on each type of MSN in these studies was characterized by combining LC-MS and TGA data. Protein was released from the particles for analysis using a typical denaturation process (see ESI†). The amount of protein released by this technique was consistent with the TGA data, as confirmed by the bicinchoninic acid (BCA) assay. While other studies have shown the wide range of proteins that adsorb onto the surfaces of various types of nanoparticles, most of these results have been presented in terms of relative amounts of each. For example, Monopoli *et al.*[16] applied a normalization to the spectral counts obtained from LC-MS data that took into account the molecular weight of each protein, but this does not describe the mass of each adsorbed protein. Consequently, in these studies, spectral counts from LC-MS experiments were normalized to obtain the relative percentages of each protein on the surface, and this value was then multiplied by the weight of protein determined by TGA to obtain the mass of each adsorbed protein (eqn (1))

$$\frac{SpC_i}{\sum_i^n SpC_i} \times TGA \times 10 \quad (1)$$

In this equation, SpC_i is the spectral counts associated with a particular protein, and TGA is the weight percent of adsorbed protein in the particular MSN sample. The factor of 10 is added to bring the units to mg protein per g of particles. The first part of the equation is defined as normalized spectral counts, abbreviated NSpC. SpC values and a heat map of the complete set of adsorbed proteins for unmodified, $-NH_2$ modified, and –COOH modified MSNs are, respectively, shown in Table S1 and Fig. S3,† and a subset of the most common proteins, defined as those with NSpC × TGA of 3.00 or higher, is shown in Table 2. It is apparent that although many proteins are present in 10% FBS, the subset of adsorbed proteins in each type of MSN's hard corona is much smaller.

More than 86 wt% of the adsorbed proteins was accounted for by only eight proteins (highlighted in Table 2) in the unmodified MSN sample, and the same proteins accounted for more than 60 wt% in the –COOH modified MSN sample although the total amount of adsorbed protein was significantly less. The zeta potential of the surface did not appear to be a significant factor in determining the type of protein adsorbed, because the isoelectric points (pIs) of the adsorbed proteins varied between 5.1 and 8.1. The pI values of most of the proteins

Table 2 Most common proteins found on porous 70 nm nanoparticles with various surface modifications[a]

			MSN–OH		MSN–NH_2		MSN–COOH	
Protein	Mw (kDa)	pI	NSpC[b]	NSpC × TGA[c]	NSpC	NSpC × TGA	NSpC	NSpC × TGA
Apolipoprotein A-II	11	8.10	0.248	25.1	0.194	27.9	0.140	3.21
Apolipoprotein C-III	11	5.11	0.044	4.48	0.028	4.08	0.000	0.00
Hemoglobin subunit α	15	8.44	0.000	0.00	0.045	6.48	0.024	0.55
Hemoglobin fetal subunit β	16	7.03	0.073	7.39	0.032	4.67	0.186	4.29
Hemoglobin subunit β	16	6.74	0.061	6.16	0.000	0.00	0.096	2.21
Apolipoprotein A-I-like	24	5.43	0.089	9.03	0.000	0.00	0.045	1.04
ACTA2 protein-like	26	5.24	0.060	6.06	0.000	0.00	0.010	0.24
Apolipoprotein A-I	30	5.97	0.137	13.8	0.017	2.49	0.090	2.08
Collectin-43	34	5.12	0.000	0.00	0.026	3.74	0.000	0.00
α-2-HS-glycoprotein	38	5.50	0.151	15.3	0.100	14.4	0.040	0.93
Protein AMBP	39	7.62	0.000	0.00	0.061	8.82	0.000	0.00
Actin, α skeletal muscle	42	5.23	0.037	3.75	0.000	0.00	0.015	0.35
LMW isoform of kininogen-1	48	6.62	0.000	0.00	0.025	3.58	0.000	0.00
Serum albumin	69	6.18	0.017	1.71	0.058	8.34	0.018	0.42
Prothrombin (fragment)	71	6.33	0.000	0.00	0.041	5.90	0.000	0.00
Inter-α-trypsin inhibitor heavy chain H2	106	7.94	0.000	0.00	0.043	6.21	0.007	0.16
Total protein deposit from TGA (wt%)				10.1		14.4		2.3

[a] MSN–PEG_n–OCH_3 materials did not show a weight loss from TGA and are not included here. [b] NSpC = normalized spectral counts from LC-MS, calculated as described in the text. [c] NSpC × TGA = amount of each protein found on particle, expressed as mg protein per g particles.

are below 7, so they are negatively charged at physiological pH. However, deposition on negatively charged nanoparticles does not correlate with protein charge, showing that electrostatic effects alone are not the major driving force regulating MSN–protein interactions. This is consistent with the composition of the protein corona on other particles.[20,38]

However, it is interesting to note that the molecular weights of these eight proteins were among the smallest of the entire set of identified proteins, with weights all below 38 kDa (Table 2 and Fig. S4†) because these samples all had large internal surface areas, there may be a size-exclusion effect in which larger proteins are prevented from adsorbing in large amounts by the diameter of the pores. This makes sense in light of other studies of the protein corona on dense (non-porous) silica, in which a larger fraction of the adsorbed proteins had higher molecular weights. In the case of $-NH_2$ modified MSNs the protein distribution is more varied. The eight proteins highlighted in Table 2 only account for 37 wt% of the total amount of adsorbed protein, and more proteins with higher molecular weights were adsorbed. Again, pI does not appear to play an important role here. The reason for this discrepancy could be in the dominant role of surface primary amines in the nonspecific binding of serum proteins on nanoparticles, as has been described in the literature.[39,40] Additionally, as noted above, the larger surface area of the $-NH_2$ modified MSNs indicate that the pore surfaces are more accessible to proteins, which may allow a wider variety of low molecular weight proteins to be trapped in the pores. Finally, PEGylated samples did not show any protein adsorption by LC-MS or TGA, even in the case of $-PEG_3$ modified particles with surface areas of 241 $m^2\ g^{-1}$. This confirmed the ability of PEG chains to prevent protein adsorption and therefore to prevent nanoparticle aggregation in biological medium.

In conclusion, we have characterized protein adsorption onto mesoporous silica nanoparticles (MSNs) modified with $-NH_2$, $-COOH$, $-PEG_3$, and $-PEG_{24}$ groups as well as onto unmodified MSNs, using LC-MS and TGA to determine the total mass of each protein adsorbed. The results are somewhat different from other studies performed on dense (non-porous) silica nanoparticles. Most of the adsorbed proteins had low molecular weights, and the $-NH_2$ modified MSNs had the largest variety of proteins. The pI values of the adsorbed proteins were mostly below physiological pH (7.4), although there was not a strong correlation between pI and the type of surface modification. Finally, PEGylated particles did not adsorb protein, regardless of chain length.

Acknowledgements

The authors are thankful for financial support by the Spanish Ministry of Economy and Competiveness (projects SEV-2012-0267, MAT2012-39290-C02-02 and IPT-2012-0574-300000) and by the University of Vermont.

Notes and references

1 C. L. Choi and A. P. Alivisatos, *Annu. Rev. Phys. Chem.*, 2010, **61**, 369–389.
2 A. Z. Wang, R. Langer and O. C. Farokhzad, *Annu. Rev. Med.*, 2012, **63**, 185–198.
3 M. Mahmoudi, I. Lynch, M. R. Ejtehadi, M. P. Monopoli, F. B. Bombelli and S. Laurent, *Chem. Rev.*, 2011, **111**, 5610–5637.
4 M. P. Monopoli, F. Baldelli Bombelli and K. A. Dawson, *Nat. Nanotechnol.*, 2011, **6**, 11–12.
5 D. E. Owens III and N. A. Peppas, *Int. J. Pharm.*, 2006, **307**, 93–102.
6 S. M. Moghimi, A. C. Hunter and J. C. Murray, *Pharmacol. Rev.*, 2001, **53**, 283–318.
7 P. Botella, I. Abasolo, Y. Fernandez, C. Muniesa, S. Miranda, M. Quesada, J. Ruiz, S. Schwartz Jr and A. Corma, *J. Controlled Release*, 2011, **156**, 246–257.
8 M. Lundqvist, J. Stigler, T. Cedervall, T. Berggard, M. B. Flanagan, I. Lynch, G. Elia and K. Dawson, *ACS Nano*, 2011, **5**, 7503–7509.
9 E. Casals, T. Pfaller, A. Duschl, G. J. Oostingh and V. Puntes, *ACS Nano*, 2010, **5**, 3623–3632.
10 A. L. Barran-Berdon, D. Pozzi, G. Caracciolo, A. L. Capriotti, G. Caruso, C. Cavaliere, A. Riccioli, S. Palchetti and A. Lagana, *Langmuir*, 2013, **29**, 6485–6494.
11 M. A. Dobrovolskaia, A. K. Patri, J. Zheng, J. D. Clogston, N. Ayub, P. Aggarwal, B. W. Neun, J. B. Hall and S. E. McNeil, *Nanomedicine*, 2009, **5**, 106–117.
12 M. Lundqvist, J. Stigler, T. Cedervall, G. Elia, I. Lynch and K. Dawson, *Proc. Natl. Acad. Sci. U. S. A.*, 2008, **105**, 14265–14270.
13 T. Cedervall, I. Lynch, S. Lindman, H. Nilsson, E. Thulin, S. Linse and K. A. Dawson, *Proc. Natl. Acad. Sci. U. S. A.*, 2007, **104**, 2050–2055.
14 D. Walczyk, F. Baldelli Bombelli, M. P. Monopoli, I. Lynch and K. Dawson, *J. Am. Chem. Soc.*, 2010, **132**, 5761–5768.
15 I. Lynch, A. Salvati and K. A. Dawson, *Nat. Nanotechnol.*, 2009, **4**, 546–547.
16 M. P. Monopoli, D. Walczyk, A. Campbell, G. Elia, I. Lynch, F. Baldelli Bombelli and K. A. Dawson, *J. Am. Chem. Soc.*, 2011, **133**, 2525–2534.
17 M. Ghavami, S. Saffar, B. A. Emamy, A. Peirovi, M. A. Shokrgozar, V. Serpooshan and M. Mahmoudi, *RSC Adv.*, 2013, **3**, 1119–1126.
18 A. Salvati, A. S. Pitek, M. P. Monopoli, K. Prapainop, F. Baldelli Bombelli, D. R. Hristov, P. M. Kelly, C. Aberg, E. Mahon and K. A. Dawson, *Nat. Nanotechnol.*, 2013, **8**, 137–143.
19 J. Wang, U. B. Jensen, G. V. Jensen, S. Shipovskov, V. S. Balakrishnan, D. Otzen, J. S. Pedersern, F. Besenbacher and D. S. Sutherland, *Nano Lett.*, 2011, **11**, 4985–4991.
20 S. Tenzer, D. Docter, S. Rosfa, A. Wlodarski, J. Kuharev, A. Rekik, S. K. Knauer, C. Bantz, T. Nawroth, C. Bier, J. Sirirattanapan, W. Mann, L. Truel, R. Zellner, M. Maskos, H. Schild and R. H. Stauber, *ACS Nano*, 2011, **5**, 7155–7167.
21 C. D. Walkey, J. B. Olsen, H. Guo, A. Emili and W. C. W. Chan, *J. Am. Chem. Soc.*, 2012, **134**, 2139–2147.

22 N. P. Mortensen, G. B. Hurst, W. Wang, C. M. Foster, P. D. Nallathamby and S. T. Retterer, *Nanoscale*, 2013, **5**, 6372–6380.
23 J. L. Perry, K. G. Reuter, M. P. Kai, K. P. Herlihy, S. W. Jones, J. C. Luft, M. Napier, J. E. Bear and J. M. DeSimone, *Nano Lett.*, 2012, **12**, 5304–5310.
24 T. Niidome, M. Yamagata, Y. Okamoto, Y. Akiyama, H. Takahashi, T. Kawano, Y. Katayama and Y. Niidome, *J. Controlled Release*, 2006, **114**, 343–347.
25 K. Park, *J. Controlled Release*, 2010, **142**, 147–148.
26 C. Sacchetti, K. Motamedchaboki, A. Magrini, G. Palmieri, M. Mattei, S. Bernardini, N. Rosato, N. Bottini and M. Bottini, *ACS Nano*, 2013, **7**, 1974–1989.
27 A. Jedlovszky-Hajdu, F. Baldelli Bombelli, M. P. Monopoli, E. Tombacz and K. A. Dawson, *Langmuir*, 2012, **28**, 14983–14991.
28 C. Röcker, M. Pötzl, F. Zhang, W. J. Parak and G. U. Nienhaus, *Nat. Nanotechnol.*, 2009, **4**, 577–580.
29 K. Prapainop, D. P. Witter and P. Wentworth Jr, *J. Am. Chem. Soc.*, 2012, **134**, 4100–4103.
30 M. Vallet-Regi, F. Balas and D. Arcos, *Angew. Chem., Int. Ed.*, 2007, **46**, 7548–7558.
31 I. I. Slowing, J. L. Vivero-Escoto, C. W. Wu and V. S. Lin, *Adv. Drug Delivery Rev.*, 2008, **60**, 1278–1288.
32 Y. Chen, H. Chen and J. Shi, *Adv. Mater.*, 2013, **25**, 3144–3176.
33 D. Tarn, C. E. Ashley, M. Xue, E. C. Carnes, J. I. Zink and J. Brinker, *Acc. Chem. Res.*, 2013, **46**, 792–801.
34 B. G. Trewyn, C. M. Whitman and V. S.-Y. Lin, *Nano Lett.*, 2004, **4**, 2139–2143.
35 F. Gao, P. Botella, A. Corma, J. Blesa and L. Dong, *J. Phys. Chem. B*, 2009, **113**, 1796–1804.
36 J. L. Vivero-Escoto, I. I. Slowing, B. G. Trewyn and V. S.-Y. Lin, *Small*, 2010, **6**, 1952–1967.
37 Q. He, J. Zhang, J. Shi, Z. Zhu, L. Zhang, W. Bu, L. Guo and Y. Chen, *Biomaterials*, 2010, **31**, 1085–1092.
38 S. Tenzer, D. Docter, J. Kuharev, A. Musyanovych, V. Fetz, R. Hecht, F. Schlenk, D. Fischer, K. Kiouptsi, C. Reinhardt, K. Landfester, H. Schild, M. Maskos, S. K. Knauer and R. H. Stauber, *Nat. Nanotechnol.*, 2013, **8**, 772–781.
39 M. A. Dobrovolskaia, P. Aggarwal, J. B. Hall and S. E. McNeil, *Mol. Pharmaceutics*, 2008, **5**, 487–495.
40 J. L. Towson, Y.-S. Lin, J. O. Agola, E. C. Carnes, H. S. Leong, J. D. Lewis, C. L. Haynes and C. J. Brinker, *J. Am. Chem. Soc.*, 2013, **135**, 16030–16033.

